RSC Advances

ROYAL SOCIETY OF CHEMISTRY

www.rsc.org/advances

A table of contents entry

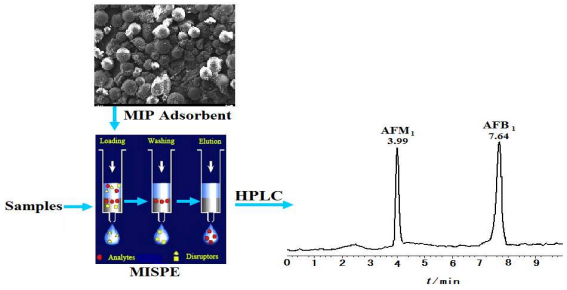

Molecularly imprinted solid phase extraction for determination of aflatoxin M_1 and B_1 in foods and feeds.

Molecularly Imprinted Solid Phase Extraction Coupled to High Performance Liquid Chromatography for Determination of Aflatoxin M_1 and B_1 in Foods and Feeds

Shoulian Wei *, Yong Liu, Zijun Yan, Ling Liu*

Faculty of Chemistry and Chemical Engineering, Zhaoqing University, Zhaoqing 526061, P.R. China

Correspondence to: Shoulian Wei (Email: weishlmary@126.com) or Ling Liu (Email: lingliu0813@163.com)

Abstract A molecularly imprinted polymer was synthesized by a miniemulsion polymerization method using aflatoxin B_1 as the molecular template, methacrylic acid (MAA) as the functional monomers, ethylene glycol dimethacrylate as the cross-linker, span80 and hexadecyl trimethyl ammonium bromide as the surfactants and n-hexadecane as the hydrophobic reagent in the presence of water. This imprinted polymer was characterized by FT-IR, ^{1}H NMR, scanning electron microscopy, laser light scattering and adsorption experiments, in which the results showed good recognition and selectivity to aflatoxin B_1 and M_1. Using the prepared polymer as a solid phase extraction sorbent, a highly selective sample pre-treatment method combined with high performance liquid chromatography and fluorescence detection was developed for determination of aflatoxin B_1 and M_1 in foods and feeds. The limit of detection and limit of quantification of this method for aflatoxins M_1 and B_1 were 0.05 $\mu g \cdot kg^{-1}$ and 0.16 $\mu g \cdot kg^{-1}$, respectively. The average recovery values from barley, peanut oil, feed and beer spiked samples ranged from 83% to 96%. The precision ranged from 2.2% to 5.6% for these samples. The proposed method was found to be more effective and economical as a pre-treatment technique than regulation 2006/40/EC.

1. Introduction

Aflatoxins (AFs) belong to a group of closely related hepato-carcinogenic bisdihydrofurano metabolites produced by certain species of *Aspergillus*, specifically *Aspergillus flavus* and *Aspergillus parasiticus* [1-2]. *Aspergillus flavus* produces only aflatoxin B, whereas *Aspergillus parasiticus* produces both B and G [3]. Among them, aflatoxin B_1 (AFB_1), the most common and most toxic, has been found to cause human hepatocellular carcinoma and has been classified as a group 1 human carcinogen by the International Agency for Research on Cancer (IARC) in 1993 [4]. Due to their frequent occurrence and potential threat to human health and animals, the European

Commission Regulation 2010/165/EC was therefore established and allows for a maximum residue limit of 8 $\mu g \cdot kg^{-1}$ for AFB_1 in foodstuffs [5]. Barley, rice, peanut oils, beer and feeds have been found to be contaminated with AFB_1 [6-7]. To continuously monitor AFB_1 levels in these foodstuffs, a sensitive, economical and accurate method is necessary.

Several analytical methods for the determination of AFB_1 in foods and feeds include thin layer chromatography [8], enzyme-linked immunosorbent assays [9], biosensor [10-11], capillary electrophoresis [12] and high performance liquid chromatography (HPLC) [13-15]. Among them, an immunoaffinity clean-up step and HPLC with pre-column derivation, and fluorescence detection is often used for routine screening. Immunoaffinity sorbents, based on molecular recognition by antibodies, exhibit high selectivity to target molecules, however, they also display instability, are difficult to prepare, and have a relatively high cost. Therefore, the development of a selective, stable, and economical sorbent material is crucial.

Molecularly imprinted polymers (MIPs) are tailor-made polymers with a predetermined selectivity toward a given analyte or a group of structurally related species [16-17]. MIPs are prepared by the polymerization of suitable functional monomers and cross-linking agents in the presence of a molecular template. After polymerization, the template is removed from the polymeric matrix leaving cavities complementary in size and shape to the template. MIPs with binding sites hold many advantages over natural antibodies, including storage stability, low cost, ease of preparation and reusability. Because of these advantages, MIPs are widely used in many different applications, such as affinity separation [18-19], catalysis [20-21], solid-phase extraction (SPE) [22-24], drug release [25] and sensors [26-27]. Recent developments have demonstrated that applications of MIPs as SPE sorbents are the most advanced application area of MIPs and are good alternatives to immunoaffinity sorbents [28-29]. To the best of our knowledge, AF molecularly imprinted polymers have not been prepared or employed as SPE sorbents for elimination of AFs from grains, foods and feed samples.

The MIPs used as SPE sorbents are usually prepared by bulk polymerization [30-31]. However, it is known that the obtained imprinted polymers are blocks that need to be crushed, ground and sieved to get appropriate polymeric particles. The whole process is tedious and time-consuming, and the shapes and sizes of the obtained particles are usually irregular, resulting in low adsorption capacity and decreased of selectivity.

To address these concerns, a simple molecularly imprinted nanosphere for AFB_1 was prepared by a miniemulsion polymerization method and applied in SPE coupled with pre-column derivation and HPLC-FLD. This method was developed and optimized for the determination of AFM_1 and AFB_1 in barley, beer, peanut oil, and feed samples. The imprinting performance of the AFB_1 imprinted nanospheres was evaluated for adsorption capacity and selectivity. The factors affecting the extraction of AFB_1 were optimized, and the validation and applicability of this method was evaluated. Compared with an immunoaffinity column, the proposed MISPE column provides a rapid, sensitive, and reliable method for analysis of AFM_1 and AFB_1 in grains, foods, and feed samples.

2. Experimental

2.1. Materials and reagents

AFB_1 and AFM_1 (5.0 mg) were purchased from Sigma Chemical (St Louis, MO, USA). Methacrylic acid (MAA) was obtained from Tianjin Kermel Chemical Reagent Co., Ltd, China. Ethylene glycol dimethacrylate (EGDMA) was purchased from Aladdin Chemistry Co., Ltd, China. 2, 2'-azobisiso - butyronitrle (AIBN) was supplied by Tianjin Baishi Chemical Industry Co., Ltd, China. Methanol and acetonitrile (chromatographic grade) were purchased from Tianjin Chemical Reagent Factory (Tianjin, China). Ultrapure water was purified on a Milli-Q system (Millipore Co., USA). All other reagents were analytical-grade and purchased from Guangzhou Chemical Reagent Factory (Guangzhou, China). Northwest barley and Jiangsu barley were obtained from State Farms malt Co., Ltd (Jiangsu province, China). Australian barley was obtained from Cofco Corporation, China. Peanut oil, beer, and feeds were purchased from the local market.

2.2. Instrumentation

HPLC analysis was carried out on an Agilent 1200 LC system (Agilent, Germany) equipped with a fluorescence detector (FLD) and a TC-C_{18} column (250 mm × 4.6 mm i.d., 5 μm packing). Excitation and emission wavelengths were set at 365 nm and 440 nm, respectively. Pre-column derivatization with trifluoroacetic acid to form a fluorescent intermediate was used to enhance fluorescence intensity. The mobile phase for HPLC experiments was acetonitrile-water (75:25, v/v), with a flow rate of 1.0 $mL \cdot min^{-1}$. The injection volume was 20 μL, and column temperature

was kept at 30 °C. Immunoaffinity columns (AflaTest) were supplied by Vicam (Watertown, MA, USA). Scanning electron microscopy (SEM) was performed on a Philips XL-30 (Japan). FTIR spectra were recorded with a Shimadzu model FTIR-84003 spectrophotometer. Particle size was measured by laser light scattering analyser (Mastersizer, 2000，Malvern, England). ^{1}H NMR spectra measurements were executed on a VARIAN Mercury-Plus 300 NMR spectrometer operating at 250 MHz, using deuterated dimethyl sulfoxide (DMSO-d6) as solvent and tetramethylsilane (TMS) as an internal standard. The temperature was 25 °C.

2.3. Emulsion preparation

Fifty mL of a 1% emulsion (mass ratio of 3:7 /Span80: CTAB, 0.8 mmol n-hexadecane) was sonicated for 20 min with an ultrasonic sonicator to form a stable emulsion.

2.4. Preparation of molecular imprinted polymers with emulsion methods

1.56 mg of AFB_1, 1.72 mg of the functional monomer MAA, 19.82 mg of the cross linking agent EGDMA, and 5 mL of chloroform were added to a flask. The mixture was sonicated for 5 min and vented with N_2 for 5 min. The mixture was placed slowly into a reactor containing 50 mL of emulsion, and sonicated for 20 min to form a miniemulsion. Then, 5 mg AIBN was added to the reactor and polymerization was achieved at 75 °C for 17 h under a nitrogen atmosphere with stirring at 400 rpm. Afterwards, the polymer microspheres were filtered and washed with dd-H_2O and ethanol. In order to remove the template and residues of nonreactive species, the microspheres were taken into a soxhlet apparatus and refluxed with methanol–acetic acid (9:1, v/v) until no AFB_1 was detected by HPLC. Finally, the microspheres were rinsed with water and dried at 60 °C in an oven for 12 h. The non-imprinted polymer microspheres (NIPs) were prepared using the same procedure but without AFB_1.

2.5. Binding experiments

10 mg of either MIPs or NIPs was placed into centrifuge tubes and mixed with 2 mL acetonitrile/water (85:15, v/v) solution containing various concentrations (40, 80, 120, 160, 200 and 240 $\mu g \cdot mL^{-1}$) of AFB_1. The mixture was shaken for 1 h at room temperature, centrifuged, and filtered. The free concentration of AFB_1 after adsorption was determined by HPLC. Based on the change in concentration of AFB_1 in solution before and after binding, the adsorption capacity value Q of nanospheres for AFB_1 were calculated by Eq. (3)

$$Q = (C_0 - C_e) \times V/m \quad (3)$$

where C_0 and C_e are the initial and equilibrium concentration of AFB_1, respectively, V is the volume of the solution, and m is the mass of nanospheres.

2.6. Selectivity experiment

In order to evaluate the selective recognition ability, AFM_1 and griseofulvin (GRI) were selected as competitive agents to estimate selectivity of the imprinted nanospheres for AFB_1. 10 mg of MIPs or NIPs were added, respectively, to centrifuge tubes containing 2 mL of 200 $\mu g \cdot mL^{-1}$ AFB_1, 200 $\mu g \cdot mL^{-1}$ AFM_1 and 200 $\mu g \cdot mL^{-1}$ griseofulvin mixture solutions. The mixture was shaken for 1 h at room temperature, centrifuged and filtered. Free AFB_1 and AFM_1 were determined by HPLC.

2.7. MISPE procedure

The cartridges were prepared by packing 200 mg of wet polymer into empty SPE-cartridges (Supelco, USA). The cartridges were preconditioned with 5 mL of methanol, 5 mL of methanol–acetic acid (9:1, v/v) and 5 mL of water successively. 2.0 mL of AFB_1 (6 ppb, in acetonitrile) and AFM_1 (10 ppb, in acetonitrile) mixture solution were loaded onto the cartridges at a flow rate of 2 mL min^{-1}. After loading, the cartridges were washed with 2 ml of water and centrifuged at 4000 rpm for 5 min to avoid incomplete fractions. Finally, the extracts were eluted with 3 × 2 ml of methanol/acetic acid (9:1, v/v). The elution was immediately dried at 60 °C under a nitrogen stream. The residue was dissolved in 200 μL of hexane and 100 μL of trifluoroacetic acid derivative for 30 min. After evaporation of the solution to dryness under a stream of nitrogen at ambient temperature, the residue was dissolved in 200 μL mobile phase solution for subsequent HPLC analysis.

2.8. Official method based on Immunoaffinity columns procedure

Immunoaffinity columns (IAC) procedure was performed according to the AOAC official standard method [32]. IAC column was equilibrated with 10 mL of PBS solution at a flow rate of 2–3 drops per second. After 2.0 mL of sample extract passed through it, the IAC column was washed with 15 mL dd-H_2O, and then the AFs were eluted with 2.5 mL of acetonitrile. The elution was immediately dried at 60 °C under a nitrogen stream. The residue was dissolved in 200 μL of hexane and 100 μL of trifluoroacetic acid derivative for 30 min. After evaporation of the solution to dryness under a stream of nitrogen at ambient temperature, the residue was dissolved in 200 μL mobile phase solution for subsequent HPLC analysis.

2.9. Sample extraction

The powder-type samples were extracted as follows: a 20 g sample was weighed into a 250 ml Erlenmeyer flask and extracted with 80 mL acetone-water (70 + 30) by shaking for 30 min at ambient temperature [33]. After extraction, the sample was filtered with folded filter paper. For peanut oil and beer samples, 10 g samples were extracted with 20 ml of hexane (vortexed for 2 min) and 40 ml of acetone-water (70 + 30) and combined for 30 min with shaking. After extraction and separation, a portion of the acetone-water extract was loaded on the MISPE cartridges or immunoaffinity columns. Test portions of blank samples were spiked at levels of 1.2, 2.4 and 4.8 $\mu g \cdot kg^{-1}$.

3. Results and Discussion

3.1. Extraction mechanism of MIP

Template molecule AFB_1 with functional monomer MAA based molecular imprinting was synthesized by radical polymerisation. The structural features of the AFB_1 indicate that hydrogen bonds and dipole–dipole interactions are expected to be formed between AFB_1 and MAA, whereby a carboxylic group of MAA works as a hydrogen bond acceptor interacting with oxygen atom of the AFB_1 body, respectively. The aromatic domains can provide structural elements that stabilize intermolecular complexes via $\pi-\pi$ interactions and hydrophobic association [34] (Fig. 1). After removal of the template, the cavities capable of selectively recognizing and re-binding the AFB_1 and its analogues were formed in the polymer (Fig. 1). The MIP as sorbent was packed into a SPE column while AFB_1 and its analogues in samples was extracted selectively on the MIP loaded SPE cartridges.

3.2. Characterization of MIP and NIP

The chemical structures of the obtained MIP and NIP were confirmed by ^1H NMR and FT-IR spectroscopy. ^1H NMR spectra are shown in Fig. 2. The signals at 0.8–1.2 and 1.92–2.0 ppm are ascribed to $–C–CH_3$ and $–C–CH_2–$ of the MAA unit. The signals at 3.36 ppm and 2.51 ppm are due to $O–CH_2–CH_2–O$ and $C–CH_2–C$ proton of polymer segment respectively. The –COOH active proton peak at 10–12 ppm was not detected in MIP and NIP. This is because the binding of H^+ with AFB_1 or H_2O were destroyed and can be removed during the elution process. Compared with the ^1H NMR spectra of NIP, the signals at 5.34 ppm due to –C=CH was clearly seen in MIP, indicated that AFB_1 was successfully imprinted in the polymers. The molecular weight of the MIP

and NIP was calculated from the NMR spectrum by using the ratio between the peak areas at 2.51 and 1.2. The number-averaged molecular weight of the MAA-EGDMA-EGDMA (NIP) and MAA-EGDMA-EGDMA-AFB_1 (MIP) copolymer of 9% and 21% MAA weight content was determined to be 2272.6 and 2463.6, respectively.

FTIR spectra of MIP and NIP are shown in Fig. 3. The wide and strong absorption bands at about 3518 cm^{-1} and 953 cm^{-1} were due to the stretching vibrations of –OH groups from MAA. Vibration bands of CH_3 were observed at about 2984, 2947, 1453 and 1387 cm^{-1}, respectively. The strong absorption bands at 1726 cm^{-1} indicated the existence of carbonyl functional groups (–COO) from EGDMA and MAA. MIP have very weak C=C vibrations at 1625 cm^{-1}, suggesting that the C=C double bond is broken after polymerization. The strong absorption bands at 1257 cm^{-1} and 1162 cm^{-1} indicated the existence of C–O stretching vibrations in the polymers. Compared with the infrared data of NIP, the absorption peaks of MIP at 3518, 1162 and 953 cm^{-1} corresponding to NIP, showed a slight drift. This indicated that the hydrogen bonds of alpha methyl acrylic acid with molecular template in the MIP were destroyed (Fig. 1), thus causing the electron cloud density of methyl acrylic acid to increase. This, in turn, increased the force constant of the bond, leading to a vibrational frequency shift toward the high frequency end of the spectrum. MIP was thus successfully synthesized based on this hydrogen bonding interaction.

The SEM images shown in Fig. 4 revealed that MIP and NIP were regular, spherical with a rough surface, and displayed good dispersion, which is conducive for rapid binding of template molecules. The particle size distribution and average particle size of the microspheres was measured by laser light scattering shown in Fig. 5. The particle size distribution of the MIP and NIP was found to be between 44 and 189 μm, and between 24 and 162 μm, respectively. The average particle size of the MIP and NIP was 108.5 and 98.6 μm, respectively. The obtained MIP and NIP particles with a rather broad size distribution may be attributed to the uneven stirring speed and reaction temperature fluctuations during polymerization, which results in emulsion droplets with size differences. However, the morphology of MIP and NIP and the average particle size showed no significant differences, indicating its adsorption selectivity differences are mainly caused by imprinting effects.

3.2. Adsorption isotherm

It is important to investigate the adsorption capacity of the imprinted nanospheres. Binding experiments were performed as described in Section 2.5. The adsorption isotherms of MIP and NIP to AFB_1 are plotted in Fig. 6, and shows that the binding capacity of MIP increased with increasing concentration of AFB_1 until it reached an equilibrium state, which is greater than that of NIP. The maximum, Q_{max}, adsorption of MIP and NIP for AFB_1, was estimated to be 8.2 $mg \cdot g^{-1}$and 4.9 $mg \cdot g^{-1}$, respectively. The static adsorption capacity of MIP was about two times that of NIP. The results indicated that MIP has a good imprinting effect to AFB_1 and is a potential sorbent to enrich tracing of AFB_1 in complicated samples.

3.3. Adsorption selectivity

AFM_1 and GRI were chosen as species for the competitive recognition research. The adsorption amounts, Q_e, were examined as described in Section 2.6. The distribution coefficient (K_d), selectivity coefficient (k) and the relative selectivity coefficient (α) of the sorbent were calculated by the following formulas

$$K_d = \frac{Q_e}{C_e}, \quad (2)$$

$$k = \frac{K_d(\mathrm{AFB_1}\ or\ \mathrm{AFM_1})}{K_d(\mathrm{GRI})}, \quad (3)$$

$$\alpha = \frac{k_{MIP}}{k_{NIP}}, \quad (4)$$

where C_e ($mg \cdot L^{-1}$) is the equilibrium concentration of AFB_1 or AFM_1. The results are shown in Table 1. K_d and k values of MIP are clearly larger than that of NIP. The relative selectivity coefficients of AFB_1 and AFM_1 were 1.6 and 1.4, respectively, and possibly due to MIP offering more specific recognition sites for the template AFB_1 and its structural analogues AFM_1. These results indicated that MIP has a strong binding ability and high selectivity for the template molecule AFB_1 and its structural analogues AFM_1.

3.4. Desorption and reusability

To investigate the reusability of the MIP sorbents, the adsorption–desorption cycle was checked 10 times using the same MIP sorbents with methanol–acetic acid (9:1, v/v) as the eluting solvent. It was found that the adsorption capacity of MIP for AFB_1 and AFM_1 remained essentially the same as cycle number increased from 1 to 6. After cycle number 6, however, the adsorption capacity of MIP for AFB_1 and AFM_1 slowly decreased. After ten cycles, the adsorption capacity of MIP for AFB_1 and AFM_1 decreased by 11.6% and 14.8%, respectively, indicating that MIP had

good reusability and stability for AFB_1 and AFM_1 adsorption.

3.5 Optimization of the MISPE procedure

The development of a separation and enrichment process was crucial for detecting relatively low concentrations of analytes contained in complex samples. MISPE was the most effective method for the separation and enrichment of the target analytes and the process was optimized with respect to loading sample pH, flow rate, washing solvent and type and volume of the eluting solvent.

The effect of the loading sample pH was investigated within a pH range from 3 to 9. The results show that the adsorption capacity of MIP for AFB_1 and AFM_1 increased with increasing pH from 3 to 6 and then gradually decreased for pH values from 7 to 9. This might be attributed to the binding of H^+ with AFB_1 or AFM_1 at a low pH, which hindered the combination of AFB_1 or AFM_1 with MIP. Above pH 7, small amounts of AFB_1 or AFM_1 bound due to the degradation of AFB_1 or AFM_1. Thus, a pH of 6.5 was chosen as the optimum loading sample pH.

Different washing solvents, consisting of 5% methanol-water, 10% methanol-water and 20% methanol-water, were selected for this study. As shown in Fig. 7, the best results were obtained with a 10% methanol-water solution. This is probably due to the fact that higher concentrations of methanol (greater than 10%) can wash out different polar interfering compounds, although it may wash out analytes to a certain extent as well. Additionally, washing volume was investigated from a range of 1 mL to 8 mL. The results indicated that washing with a 2 × 2 mL of 10% methanol-water solvent had no obvious effect on the retention of AFB_1 and AFM_1 on MIP cartridges. Beyond 4 mL, the recovery of AFB_1 and AFM_1 on the MIP cartridge gradually decreased. Thus, a 2 × 2 mL of 10% methanol-water was selected for washing interfering compounds.

The influence of different eluent solvents was also investigated in order to examine the desorbing properties of AFB_1 and AFM_1 from the sorbent (Table 2). It was determined that an increase in methanol and acetic acid in the elution solution, increased the recovery of AFB_1 and AFM_1 in the MIP cartridge. The best results were obtained for 4 mL of methanol- acetic acid（9:1, v/v). This may be because acetic acid competed with AFB_1 and AFM_1 for MIP in the binding sites and methanol was able to decrease the non-specific interactions between MIP and the two target analytes. The effect of different volumes of eluent (1.0, 2.0, 4.0, 6.0 and 8.0 mL) was also studied.

The results are shown in Fig. 8. The recovery of AFB_1 and AFM_1 increased to 96.4% and 91.9%, respectively, by increasing the volume of eluent up to 6.0 mL and then remained constant. Thus, 6.0 mL of volume was selected for the elution step.

The effect of loading sample flow rate was investigated in the range of 0.5 $mL \cdot min^{-1}$ to 4 $mL \cdot min^{-1}$. The results showed that for flow rates higher than 2.0 $mL \cdot min^{-1}$, the recoveries continuously decreased due to the decreased contact time of analytes with the MIP adsorbent. Therefore, 2.0 $mL \cdot min^{-1}$ was chosen as the optimal sample flow rate. The flow rate of eluent solvent was also studied from the range of 0.5 $mL \cdot min^{-1}$ to 4 $mL \cdot min^{-1}$. Maximum recovery was obtained in the range of 0.5 $mL \cdot min^{-1}$ to 1.0 $mL \cdot min^{-1}$. For flow rates higher than 1.0 $mL \cdot min^{-1}$, the recoveries decreased, as the analyte was not completely eluted from the packed column bed. Thus, a 1 $mL \cdot min^{-1}$ flow rate was selected as the optimum eluting flow rate.

3.6. Comparison of retention behaviour of the immunoaffinity column and the MISPE column

Chromatograms of the spiked Australia barley extraction solution from both the immunoaffinity and MISPE columns are shown in Fig. 9. The spike level was 2.4 ppb for aflatoxins M_1 and B_1. Fig. 9A shows the extraction solution obtained from the immunoaffinity column and Fig. 9B shows the results from the MISPE column. The retention times at 3.99 min and 7.64 min were identified as AFM_1 and AFB_1, respectively. It was found that AFM_1 and AFB_1 were retained well for both the immunoaffinity and the MISPE columns. Moreover, the matrix compounds were removed more so for the MISPE column than for the immunoaffinity column. The recoveries of AFM_1 and AFB_1 were 92.8% and 93.5% on the immunoaffinity column, respectively, and 92.1% and 93.3% for the MISPE column. These results demonstrated that the MISPE column can be used as a substitute for the immunoaffinity column for effective removal of complicated matrix molecules.

3.7. Method validation

A method based on MISPE coupled to HPLC was established. Using the determined optimum conditions, an external aqueous calibration and standard addition calibration of a blank sample extract were constructed containing AFB_1 and AFM_1 between 0.2 ppb to 20 ppb ($\mu g \cdot L^{-1}$) in order to study possible matrix effects. The calibration equation in aqueous solution was $y = 17564c_{AFM1}–540$ ($R^2 = 0.9996$) and $y = 17641c_{AFB1}–807$ ($R^2 = 0.9998$) for AFM_1 and AFB_1,

respectively. The calibration equation in extract was $y = 17189c_{AFM1}–282$ ($R^2 = 0.9994$) and y = $17296c_{AFB1}–756$ ($R^2 = 0.9995$) for AFM_1 and AFB_1, respectively. There were no significant differences in the calibration curves for both AFB_1 and AFM_1 obtained in aqueous and in the matrix solutions. The results showed that the matrix could be efficiently removed during the MISPE pre-concentration stage. Therefore, the external aqueous calibration can be used to determine AFB_1 and AFM_1 in practical samples after the MISPE pre-concentration procedure.

Limit of detection (LOD) and limit of quantification (LOQ) were calculated according to LOD = (3*SD)/m and LOQ = (10*SD)/m, where SD is the standard deviation of 10-replicate measurements on a procedural blank (Milli-Q water treated as a sample), and m is the slope of the external aqueous calibration curve. The LOD of AFM1 and AFB1 was 0.05 $\mu g \cdot kg^{-1}$. Similarly, the LOQ was found to be 0.16 $\mu g \cdot kg^{-1}$ for AFM1 and AFB1. These LOD and LOQ values are similar to reports from Chun [35] using HPLC with a fluorescence detector (0.08 $\mu g \cdot kg^{-1}$ and 0.15 $\mu g \cdot kg^{-1}$ for AFB1) and are slightly less sensitive than what Manetta and Baltaci reported in previous literature reports [12, 36] (5 $ng \cdot kg^{-1}$ for AFM1, 0.02 $\mu g \cdot kg^{-1}$ and 0.07 $\mu g \cdot kg^{-1}$ for AFB1). However, this developed method using a preliminary MISPE column replacing an immunoaffinity column as a purification step reduces cost. Moreover, the detection limit is far below the current legal national standard limit in China. So the proposed method is feasible for determination of AFM_1 and AFB_1 in foods and feeds.

Accuracy of the overall procedure was evaluated by the determination of the recoveries of four blank samples spiked with aflatoxins M_1 and B_1 at concentrations of 1.2, 2.4 and 4.8 ppb. Precision was assessed by analyzing a spiked sample six times and was expressed as the relative standard deviation (RSD). The results are presented in Table 3. The obtained recovery values and RSD from the four spiked samples ranged from 83% to 96% and from 2.2% to 5.6%, respectively, indicating that the developed method is accurate enough for determining AFM_1 and AFB_1 in food samples.

3.8. Application

To demonstrate the application of our method, barley, peanut oil, beer and feed samples (section 2.8) were tested. The results are listed in Table 3. The AFM_1 contamination was not detected in all samples tested. The AFB_1 contamination was not detected in barley, peanut oil, or beer samples, but was detected in feed. The typical chromatograms of naturally contaminated

corn feed samples are shown in Fig. 10. Retention time at 7.67 min was identified as AFB_1. Four feed samples out of six (66.7% incidence) were contaminated with AFB_1 and 1 feed sample (16.7% incidence) was over 10 $\mu g \cdot kg^{-1}$, which is the feed hygiene standard (GB13078-2001) tolerance limit for AFB1 in China. High detection rates and high levels of AFB_1 in feed samples indicated the need for routine monitoring to maintain AFB_1 to the lowest possible levels.

4. Conclusion

In this study, AFB_1-imprinted MIPs were successfully synthesized by a miniemulsion polymerization method and used as sorbents for MISPE of food and feed samples. The sorbent exhibited strong binding ability, high selectivity, good reusability and stability. Under optimized MISPE conditions, the cartridge showed high extraction efficiency and removed matrix interferences from real samples efficiently, suggesting that it can be employed as a substitute to immunoaffinity columns for sample purification steps in the detection of aflatoxin. The developed MISPE coupled with HPLC-FLD showed low detection limits, high precision, a high degree of accuracy, and can serve as a monitoring system for aflatoxin (M_1 and B_1) contamination in a variety of food and feed samples in a cost-saving manner (immunoaffinity column not required).

Acknowledgements

This work is financially supported by the Science and Technology Innovation Project of Guangdong provincial education department (No. 2012kjcx0104 and No. 2013kjcx0194), the Science and Technology Planning Project of Zhaoqing City, Guangdong province (No. 2013C019) and the Natural Science Foundation of Guangdong Province (No. S2012040007710).

References

1 T. Yoshinari，S. Sakuda，M. Watanab，Y. Kamata，T. Ohnishi and Y. Sugita-Konishi, *J. Agr. Food Chem.,* 2013, **61**, 7925.

2 R. Zivoli，L. Gambacorta，G. Perrone and M. Solfrizzo, *J Agr. Food Chem.*, 2014, **62**, 5707.

3 E. E. Creppy, *Toxicol. Lett.*, 2002, **127**, 19.

4 International Agency for Research on Cancer (IARC). *IARC monographs on the Evaluation of Carcinogenic Risk to Humans*, 1993, **56**, 245.

5 Commission Regulation (EU) No 165/2010 of 26 February 2010 amending Regulation (EC) No 1881/2006 setting maximum levels for certain contaminants in foodstuffs as regards aflatoxins.

6 X. Lai, R. Liu, C. Ruan, H. Zhang and C. Liu, Food Control, 2015, 50, 401.

7 K. Benešová, S. Běláková, R. Mikulíková and Z. Svoboda, Food Control, 2012, 25, 626.

8 S. Vijayanandraj，R. Brinda，K. Kannan，R. Adhithya，S. Vinothini，K. Senthil，R. R. Chinta，V. Paranidharan and R. Velazhahan, *Microbiol. Res.*, 2014, **169,** 294.

9 Y. K. Wang， Y. X. Yan， S. Q. Li， H. A. Wang， W. H. Ji and J. H. Sun, *J Agr. Food Chem.*, 2013, **61**, 10948.

10 M. Campas, D. Garibo and B. Prieto-Simon, *Analyst*, 2012, **137**, 1055.

11 M. Zangheri, F. D. Nardo, L. Anfossi, C. Giovannoli, C. Baggiani, A. Roda and M. Mirasoli, *Analyst*, 2015, **140**, 358.

12 R. Peña, M. C. Alcaraz, L. Arce, A. Ríos and M. Valcárcel, *J. Chromatogr. A,* 2002, **967,** 303.

13 H. Wang, L. Zhao，H. M. Yang，Q. L. Guo，H. L. Shi，H. Y. Pan，L. P. Zhao and Qian C. *Anal. Methods,* 2014, **6**, 1545.

14 M. Hashemi and Z. Taherimaslak, *Anal. Methods*, 2014, **6**, 7663.

15 W. S. Khayoon and B. Saad, *Food Chem.*, 2010, **118**, 882.

16 X. Gao， W. Y. Cao， M. M. Chen， H. Y. Xiong， X. H. Zhang and S. F. Wang, *Electroanal.*, 2014, **26**, 2739.

17 17 X. Ma， W. Ji， L. Chen， X. Wang， J. Liu and X. Wang, *J Sep. Sci.*, 2014, DOI: 10.1002/jssc.201400911.

18 K. Nemoto, T. Kubo, M. Nomachi, T. Sano, T. Matsumoto, K. Hosoya, T. Hattori and K. Kaya, *J. Am. Chem. Soc.*, 2007, **129**, 13626.

19 R. E. Fairhurst, C. Chassaing, R. F. Venn and A. G. Mayes, *Biosens. Bioelectron.*, 2004, **20**, 1098.

20 J. P. Ferreira，R. Viveiros，A. Lourenço，S. M. Soares，A. Rosatella and C. M. Casimiro TAfonso, *RSC Adv.*, 2014, **4**, 54948.

21 W. Q. Sun，R. Tan，W. G. Zheng and D. H. Yin, *Chinese J Catal.,* 2013, **34**, 1589.

22 H. A. Panahi，A. Mehramizi，S. Ghassemi and E. Moniri. *J Sep. Sci.*, 2014, **37,** 691.

23 S. Manzoor，R. Buffon，A. V. Rossi. *Talanta*, 2015, **134**, 1.

24 Y. Yang，J. Yu，J. Yin，B. Shao and J. Zhang, *J. Agr. Food Chem.,*, 2014, **62**, 11130.

25 C. Y. Wang, A. Javadi, M. Ghaffari and S. Q. Gong. *Biomaterials*, 2010, **31**, 4944.

26 Y. Tong，H. Li，H. Guan，J. Zhao，S. Majeed，S. Anjum，F. Liang and G. Xu, *Biosens. Bioelectron.*, 2013, **47**, 553.

27 R. L. Lei，C. H. Guo，H. Y. Xiong, C. Dong，X. H. Zhang and S. F. Wang. *Electroanal.*, 2014, **26**, 1004.

28 M. Wyszomirski and W. Prus, *Mol. Simulat.*, 2012, **37,** 1.

29 W. H. Ali，D. Derrien，F. Alix，C. Perollier，O. Lepine，S. Bayoudh，F. Chapuis-Hugon and V. Pichon, *J. Chromatogr. A,* 2010, **1212**, 6668.

30 N. M. Maier, G.Buttinger, S, Welhartizki, E, Gavioli and W. Lindner, *J. Chromatogr. B*, 2004, **804**, 103.

31 N. Yusof, S. Rahman, M. Hussein and N. Ibrahim, *Polymers,* 2013, **5,** 1215.

32 AOAC Official methods of analysis, Natural Toxins, AOAC, International, Gaithersburg, USA, Official Method 999.07, 18th ed., 2005, pp. 32.

33 T. Bertuzzi, S. Rastelli, A. Mulazzi and A. Pietri, *Food Anal. Methods*, 2012, **5**, 512.

34 J. Jodlbauer, N. M. Maier and W. Lindner, *J. Chromatogr. A*, 2002, **945,** 45.

35 H. S. Chun, H. J. Kim, H. E. Ok, J. B. Hwang and D. H. Chung, *Food Chem.,* 2007, **102**, 385.

36 A. C. Manetta, L. D. Giuseppe, M. Giammarco, I. Fusaro, A. Simonella, A. Gramenzi and A. Formigoni, *J. Chromatogr. A*, 2005, **1083,** 219.

Table 1 Adsorption selectivity of MIP and NIP

Adsorbate	MIP			NIP			α
	Q_e (mg·g^{-1})	K_d (mL·g^{-1})	k	Q_e (mg·g^{-1})	K_d (mL·g^{-1})	k	
AFB_1	8.2	51.6	1.98	4.9	27.9	1.26	1.6
AFM_1	7.4	45.4	1.75	4.8	27.3	1.23	1.4
GRI	4.6	26.0		4.0	22.2		

Table 2 Effect of type of eluent on AFB1 and AFM1 recovery

Eluent	Volume/mL	Recovery/%	
		AFB_1	AFM_1
methanol-water (1:3，v/v)	4	6.0%	11.5%
methanol-water (1:1，v/v)	4	9.9%	24.8%
methanol-water (9:1，v/v)	4	23.3%	38.7%
methanol-acetic acid（95:5，v/v）	4	78.8%	72.6%
methanol-acetic acid（9:1，v/v）	4	94.1%	86.9%

Table 3 The recovery values and RSD of spiked sample at three different concentration (n=6)

Samples	Analytes	Spiked ($\mu g \cdot kg^{-1}$)	Found[a] ($\mu g \cdot kg^{-1}$)	Recovery（%）	RSD (%)
Barley	AFM_1	1.2	1.0±0.1	83	5.6
		2.4	2.2±0.1	92	4.5
		4.8	4.5±0.2	94	3.5
	AFB_1	1.2	1.1±0.0	92	4.5
		2.4	2.2±0.1	92	3.6
		4.8	4.5±0.2	94	3.3
Peanut oil	AFM_1	1.2	1.0±0.0	83	4.7
		2.4	2.2±0.1	92	4.5
		4.8	4.4±0.2	92	3.8
	AFB_1	1.2	1.1±0.0	92	5.5
		2.4	2.2±0.1	92	4.1
		4.8	4.5±0.2	94	3.8
Feed	AFM_1	1.2	1.1±0.0	92	3.6
		2.4	2.2±0.1	92	3.6
		4.8	4.5±0.1	94	2.2
	AFB_1	1.2	1.1±0.0	92	4.5
		2.4	2.3±0.1	96	4.4
		4.8	4.5±0.2	94	3.5
Beer	AFM_1	1.2	1.1±0.0	92	4.6
		2.4	2.2±0.1	92	4.1
		4.8	4.4±0.1	92	2.9
	AFB_1	1.2	1.1±0.0	92	4.5
		2.4	2.2±0.1	92	3.6
		4.8	4.5±0.1	94	3.4

[a] Found was expressed with the mean ± standard deviation (SD)

1 Table 4 levels of aflatoxin M_1 and B_1 in real samples

Sample No.	Sample type	AFM_1	AFB_1
1	Australia barley	nd	nd
2	Jiangsu barley	nd	nd
3	Northwest barley	nd	nd
4	Luhua peanut oil	nd	nd
5	Yingmai peanut oil	nd	nd
6	Jinglongyu peanut oil	nd	nd
7	Longda peanut oil	nd	nd
8	Blue ribbon beer	nd	nd
9	Qingdao beer	nd	nd
10	Yanjing beer	nd	nd
11	Budweiser beer	nd	nd
12	Shell beans Feed	nd	5.3±0.2
13	Shell beans Feed	nd	nd
14	Corn feed	nd	7.3±0.3
15	Corn feed	nd	nd
16	Formula feed	nd	8.2±0.3
17	Formula feed	nd	11.7±0.5

2 nd: not detected

3

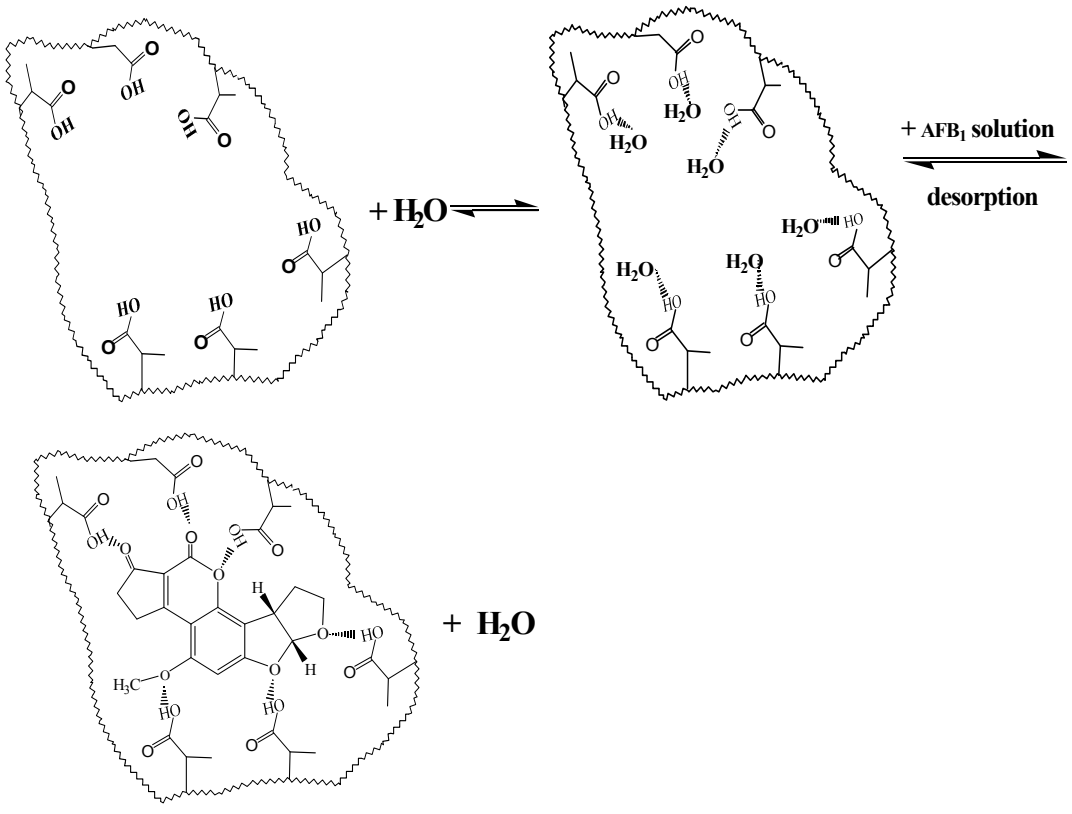

4

5

6 Fig.1 Schematic of the extraction mechanism

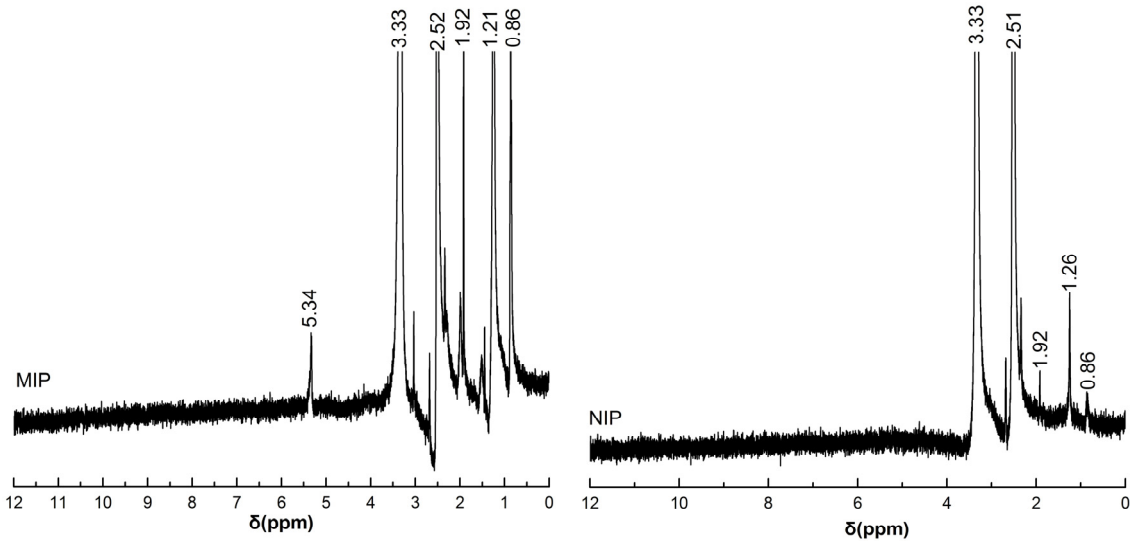

Fig.2 ^{1}H NMR spectra of MIP and NIP in DMSO-d_6

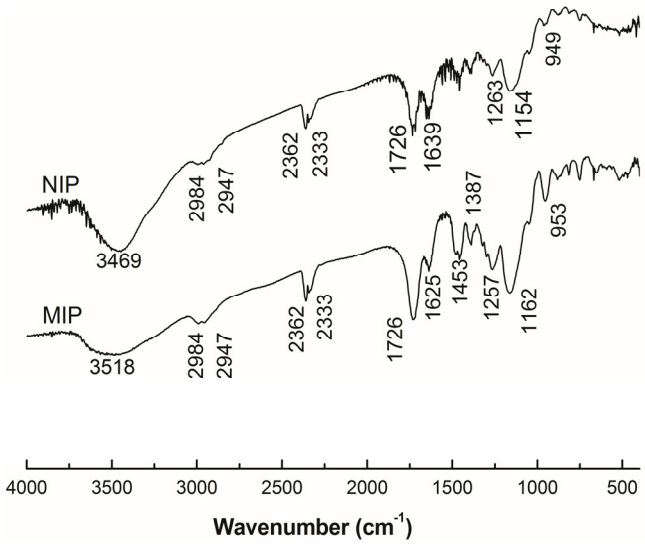

Fig.3 The FTIR spectra of MIP and NIP

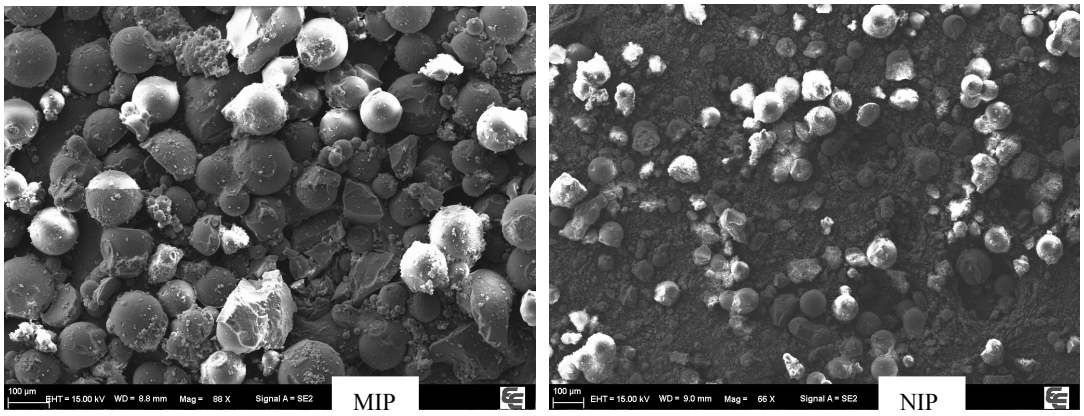

Fig.4 Scanning electron microscopy of MIP and NIP

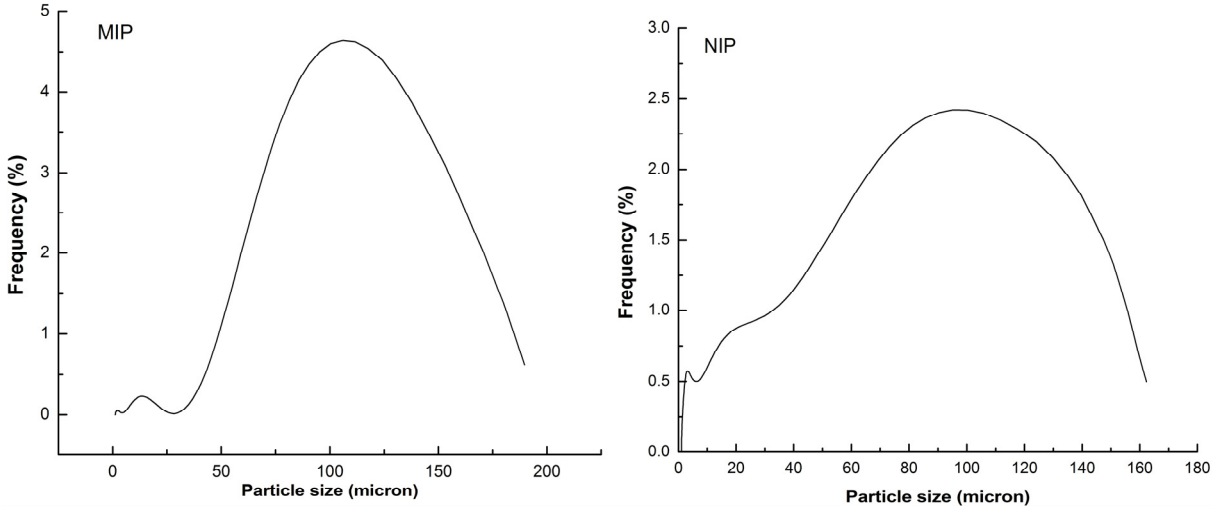

Fig. 5 The particle size distribution and mean particle size of MIPs and NIPs.

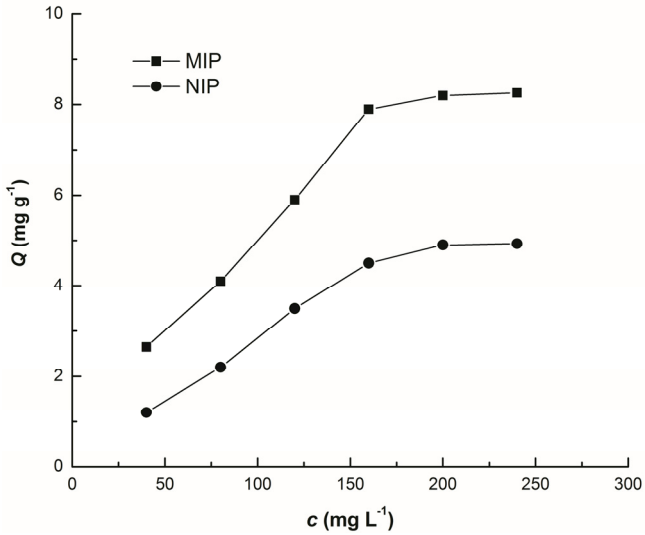

Fig. 6 Binding isotherm of MIPs and NIPs for AFB_1.

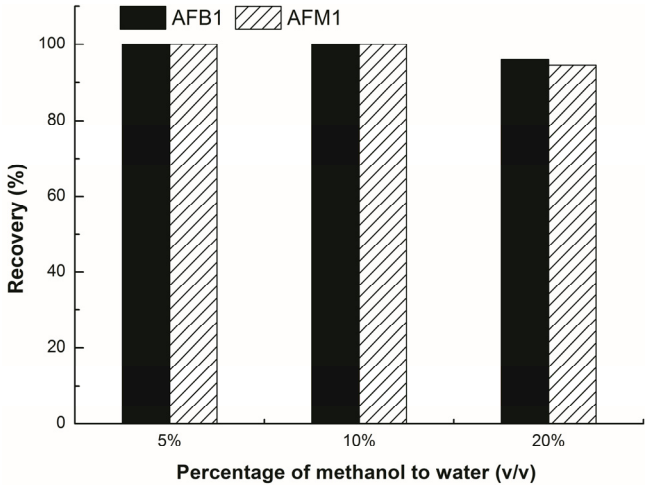

Fig. 7 The recovery of washing solution for MISPE experiment.

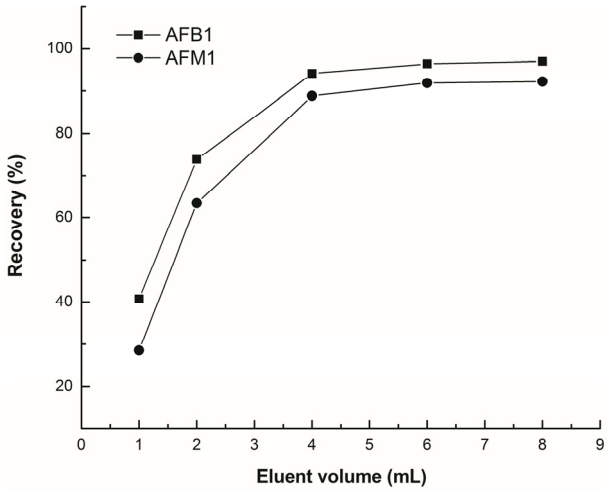

Fig. 8 Effect of the volumn of eluent

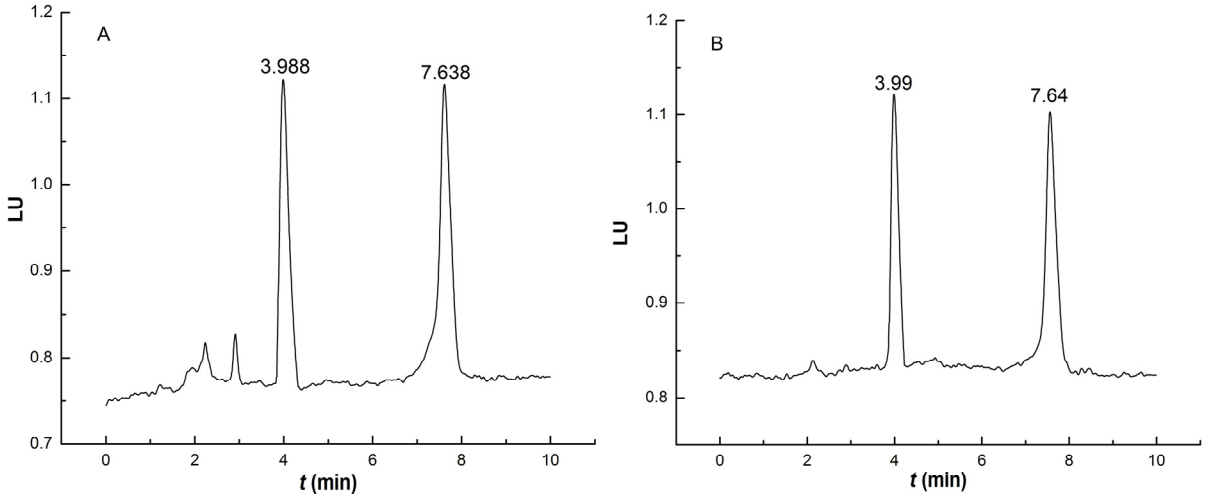

Fig. 9 Chromatograms of the spiked Australia barley sample extraction solution from the immunoaffinity (A) and MISPE column (B)

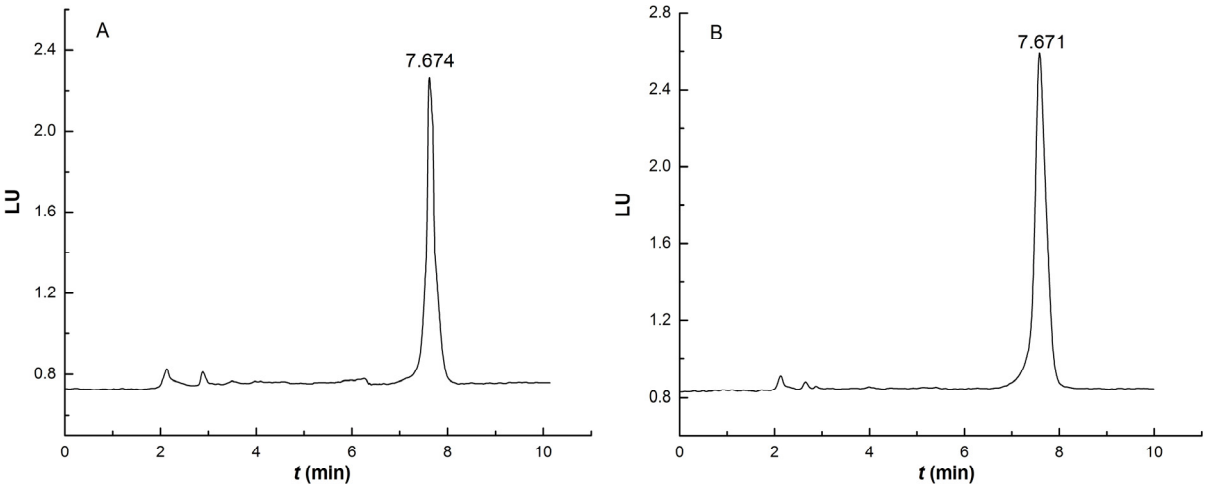

Fig. 10 Chromatograms of feed (A) and feed spiked with AFB_1 at 1.2 ppb (B)